THE JOURNAL OF BIOLOGICAL CHEMISTRY VOL. 284, NO. 5, pp. 3250–3263, January 30, 2009

MSL2 Promotes Mdm2-independent Cytoplasmic Localization of p53*

Received for publication, July 23, 2008, and in revised form, November 25, 2008 Published, JBC Papers in Press, November 25, 2008, DOI 10.1074/jbc.M805658200

Jan-Philipp Kruse and Wei Gu[1]

From the Institute for Cancer Genetics and Department of Pathology and Cell Biology, College of Physicians and Surgeons, Columbia University, New York, New York 10032

Although it was originally thought of as a passive way to block the nuclear function of p53, accumulating evidence suggests that cytoplasmic localization of p53 plays an active role in p53-mediated functions such as apoptosis and autophagy. Previous studies by us and others demonstrated that Mdm2-mediated p53 ubiquitination induces both degradation and cytoplasmic localization. Here we describe MSL2, a novel E3 ligase for p53 that promotes ubiquitin-dependent cytoplasmic p53 localization. Unlike Mdm2 or most other p53 E3 ligases, MSL2-mediated p53 ubiquitination does not affect the stability of p53. Moreover, the MSL2-mediated effect on p53 is Mdm2-independent. Thus, our study identifies an important ubiquitin-ligase for modulating p53 subcellular localization.

The function of the tumor suppressor p53 as a sequence-specific transcription factor controlling the expression of numerous target genes is critical for the regulation of cellular senescence, cell-cycle arrest, and apoptosis (1–3). During normal homeostasis, p53 is localized predominantly in the nucleus and is maintained at low levels via ubiquitination-mediated targeting for proteasomal degradation (4). Both protein levels and transcriptional activity increase dramatically in response to stress through an array of critical post-translational modifications (4, 5). Polyubiquitination of C-terminal lysines of p53 by Mdm2 (6–8) and other ubiquitin-protein isopeptide ligases (E3)[2] such as Pirh2 (9), COP-1 (10), and Arf-BP1 (11) controls p53 levels by targeting p53 for proteasomal degradation in unstressed cells or after the cellular stress is resolved (4, 12). The stress-induced p53-dependent apoptotic response consists of transcription-dependent and -independent functions of p53 (13–17). Although transactivation of pro-apoptotic target genes such as *PUMA*, *BAX*, and *PIG3* requires p53 to act as a transcription factor in the nucleus, cytoplasmic p53 can elicit an apoptotic response by localizing to the mitochondria and activating a direct mitochondrial death program (13, 18–26). Mdm2-mediated p53 monoubiquitination, occurring when Mdm2 activity levels are low, promotes p53 nuclear export and the generation of a cytoplasmic p53 pools (27–32). Once p53 localizes to the mitochondria, both directly activated and enabled pathways are utilized to induce apoptosis (18). p53 interacts with anti-apoptotic members of the Bcl family such as BclXl and Bcl2 at the outer mitochondrial membrane to release and allow the oligomerization of the pro-apoptotic factors Bak and Bax. These in turn promote the formation of pores in the mitochondrial membrane resulting in the release of cytochrome *c* and other apoptotic activators from the mitochondria (21, 22, 33–35). Alternatively, p53 can interact directly with Bak, releasing Bak from its inhibitory interaction with Mcl1 and thereby directly activating Bak-induced apoptosis (23, 36). Recently, a role for cytoplasmic p53 in autophagy was described, providing further evidence that changes on subcellular localization of p53 have profound effects on the cell (37).

Although, depending on its protein levels, Mdm2 contributes to both p53 degradation and p53 subcellular localization, all other known E3 ligases, except E4F1, have been shown to regulate only p53 degradation (4). Instead of affecting p53 levels by ubiquitination, E4F1-mediated oligoubiquitination in the hinge region has been shown to stimulate the induction of p53 target genes involved in cell cycle arrest (38). Notably, if cytoplasmic p53 localization is crucial for p53-mediated apoptosis, Mdm2 would act as a positive regulator of the p53 apoptotic response by promoting said cytoplasmic localization of p53. Such a pro-apoptotic function for Mdm2 is somewhat inconsistent with genetic data that identifies Mdm2 as the primary negative regulator of p53 (39, 40). Another interesting aspect of the role Mdm2 plays in establishing cytoplasmic p53 pools arises from data describing the localization of $p53^{QS}$, a p53 mutant unable to bind Mdm2 (41–44). Although $p53^{QS}$ localizes primarily to the nucleus, it has also been shown to be present in the cytoplasm (43), which may contribute to its apoptotic ability despite known transactivation deficiencies (42–44). p53 contains two nuclear export sequences, one in the N terminus and one in the C terminus of the protein (45, 46), as well as a C-terminal nuclear localization sequence (47). These intrinsic localization sequences contribute to a basal level of cytoplasmic shuttling of p53; however, additional factors promoting cytoplasmic p53 localization are thought to be required to explain the cytoplasmic localization and apoptotic ability of p53 mutants such as $p53^{QS}$, which cannot be regulated by Mdm2. Identifying novel mechanisms that regulate cytoplasmic p53 levels may help to explain the pro-apoptotic activity of both

* This work was supported, in whole or in part, by National Institutes of Health grants from NCI (to W. G.). The costs of publication of this article were defrayed in part by the payment of page charges. This article must therefore be hereby marked "*advertisement*" in accordance with 18 U.S.C. Section 1734 solely to indicate this fact.

[1] To whom correspondence should be addressed: 1130 St. Nicholas Ave., New York, NY 10032. Tel.: 212-851-5282; Fax: 212-851-5284; E-mail: wg8@columbia.edu.

[2] The abbreviations used are: E3, ubiquitin-protein isopeptide ligase; HA, hemagglutinin; GFP, green fluorescent protein; Ub, ubiquitin; BSA, bovine serum albumin; DPBS, Dulbecco's phosphate-buffered salt solution; siRNA, small interfering RNA; Ni-NTA, nickel-nitrilotriacetic acid; MEF, mouse embryonic fibroblast.

wild type p53 and p53 mutants such as $p53^{QS}$. Such information should provide additional insights into the extent to which both the transactivation-dependent and -independent functions of p53 contribute to its overall pro-apoptotic activity. Here, we describe a novel interacting partner for p53, MSL2 (male-specific lethal-2), which contributes to establishing cytoplasmic pools of p53-independent of Mdm2.

EXPERIMENTAL PROCEDURES

Cell Culture—H1299, 293, U2OS, and MEF $p53^{-/-}Mdm2^{-/-}$ cells were maintained in Dulbecco's modified Eagle's medium supplemented with 10% fetal bovine serum. Cells were transfected with plasmid DNA by the calcium phosphate protocol or by using Lipofectamine 2000 (Invitrogen) according to the manufacturer's protocol.

Plasmid Construction—To generate MSL2 expression constructs, the full-length MSL2 cDNA or deletion mutants were amplified by PCR from Marathon-Ready HeLa cDNA (Clontech/BD Biosciences) and subcloned into pcDNA3.1/V5-His-Topo vector (Invitrogen) or the pcDNA3.1/NT-GFP-TOPO vector (Invitrogen). Subsequently, MSL2 was subcloned into an expression vector to generate pIRES-F-HA-MSL2 for the generation of the stable line. The F-ΔRING-MSL2 construct, lacking the first 107 amino acids, was amplified by PCR from Marathon-Ready HeLa cDNA using a primer containing the FLAG sequence to generate the pTOPO-F-MSL2 Δ107 expression construct. Point mutants of p53 used in the experiments were generated using the QuikChange site-directed mutagenesis kit (Stratagene) following the manufacturer's protocol.

Immunoprecipitation and Immunoblot—Cells were transfected with FLAG-tagged expression constructs for p53 and MSL2 using the calcium phosphate method as described previously. To immunoprecipitate the ectopically expressed FLAG-tagged proteins in co-immunoprecipitation assays or from the U2OS F-HA-MSL2 stable line, transfected cells or U2OS control and U2OS F-HA-MSL2 cells lines were lysed 24 h post-transfection in BC100 buffer (20 mM Tris, pH 7.9, 100 mM NaCl, 10% glycerol, 0.2 mM EDTA, 0.5% Triton X-100 and fresh proteinase inhibitor mixture (Sigma)). For the co-immunoprecipitation experiments between F-p53 and the GFP-MSL2 subfragments, BC200 buffer (20 mM Tris, pH 7.9, 200 mM NaCl, 10% glycerol, 0.2 mM EDTA, 0.5% Triton X-100, and fresh proteinase inhibitor mixture (Sigma)) was used for cell lysis, wash steps, and elution. In all immunoprecipitations, the whole cell extracts were immunoprecipitated with the monoclonal anti-FLAG antibody-conjugated M2-agarose beads (Sigma) at 4 °C overnight. After five washes with BC100, the bound proteins were eluted using FLAG-peptide (Sigma)/BC100 for 3 h at 4 °C. The eluted material was resolved by SDS-PAGE and detected by antibodies as indicated. Whole cell lysates for inputs in ubiquitination assays and for p53 target analysis were lysed in FLAG-lysis buffer (50 mM Tris-HCl, pH 7.9, 137 mM NaCl, 10 mM NaF, 1 mM EDTA, 1% Triton X-100, 0.2% Sarkosyl, 10% glycerol, and fresh proteinase inhibitor mixture (Sigma)).

GST Pulldown Assay—GST protein and GST-p53 (FL), GST-p53(NT)-(1–73), GST-p53(M)-(100–290), and GST-p53(CT)-(290–393) were purified as described previously (48). ^{35}S-Labeled F-HA-MSL2 was prepared by *in vitro* translation using the TnT reticulocyte lysate system (Promega). 3 μg of GST protein was preincubated with *in vitro* translated F-HA-MSL2 for 3 h at 4 °C in BC100 buffer containing 0.1% Triton X-100 and 1% bovine serum albumin (BSA). GST beads were then added, and the solution was incubated overnight at 4 °C. The beads were washed, and bound protein was eluted for 1 h at 4 °C in BC100 buffer containing 0.1% Triton X-100 and 20 mM reduced glutathione (Sigma) and separated on an SDS-polyacrylamide gel for detection by autoradiography.

In Vivo Ubiquitination Assays—The p53 lysine to arginine mutants were created using the QuikChange site-directed mutagenesis kit (Stratagene) following the manufacturer's protocol. For p53 ubiquitination assays, H1299 cells plated on 100-mm dishes were transfected using the calcium phosphate method with 8 μg of pCIN4-His-HA-Ub, 2 μg of pCIN4-FLAG-p53, and 10 μg of pIRES-F-HA-MSL2 or 2 μg of Mdm2 plasmid as indicated. 24 h post-transfection cells were treated for 6 h with MG132 (20 μM) before harvesting. 10% of the cell suspension was kept for input and lysed in FLAG-lysis buffer. The remaining cells were lysed in 1 ml of buffer I (6 M guanidinium-HCl, 0.1 M Na_2HPO_4/NaH_2PO_4, 0.01 M Tris-HCl pH 8.0, 0.2% Triton X-100, 10 mM β-mercaptoethanol, and 5 mM imidazole). 30 μl of nickel-agarose beads was added, and lysates were rotated for 4 h at room temperature. The beads were then washed for 5 min at room temperature once in 1 ml of buffer I, once in 1 ml of buffer II (8 M urea, 0.1 M Na_2HPO_4/NaH_2PO_4, 0.01 M Tris-HCl pH 8.0, 0.2% Triton X-100, 10 mM β-mercaptoethanol, and 5 mM imidazole), and three times in 1 ml of buffer III (same composition as buffer II except at pH 6.3). Bound proteins were eluted in 50 μl of 2× SDS sample buffer containing 500 mM imidazole and 150 mM dithiothreitol for 30 min at room temperature and resolved on an SDS-polyacrylamide gel. Ubiquitinated p53 species were detected by Western blot using p53-specific DO-1 antibody. For MSL2 autoubiquitination assays, H1299 cells plated in 100-mm dishes were transfected with 5 μg of MSL2 expression constructs and 8 μg of pCIN4-His-HA-Ub and processed identically to the p53 ubiquitination assays.

Immunofluorescence Staining—H1299 cells were plated on glass coverslips in 6-well plates and transfected with 0.5 μg of the indicated p53 expression plasmids and 8 μg of the indicated MSL2 expression constructs using the calcium phosphate method. 24 h post-transfection, the cells were fixed with 4% paraformaldehyde for 15 min at 37 °C and then rehydrated for 5 min at room temperature with serum-free Dulbecco's modified Eagle's medium (Cellgro). The cells were then permeabilized using 0.1% Triton X-100 (Fisher) for 10 min at room temperature. Cells were then incubated with 1% BSA (Sigma)/Dulbecco's phosphate-buffered salt solution (DPBS) (Cellgro) for 1 h. Primary antibody DO-1 (Santa Cruz Biotechnology) or full-length p53 antibody (FL-393, SC-6243, Santa Cruz Biotechnology) in 1% BSA/DPBS was incubated with the cells for 1 h at room temperature and then washed with 1% BSA/DPBS for 20 min. Alexa 488-conjugated anti-mouse antibody (Molecular Probes) or Alexa 568 anti-rabbit antibody for DO-1 or 393, respectively, was added and incubated for 30 min at room temperature. Finally, after a 15-min 1% BSA/DPBS wash, the cells were counterstained with 4,6-dia-

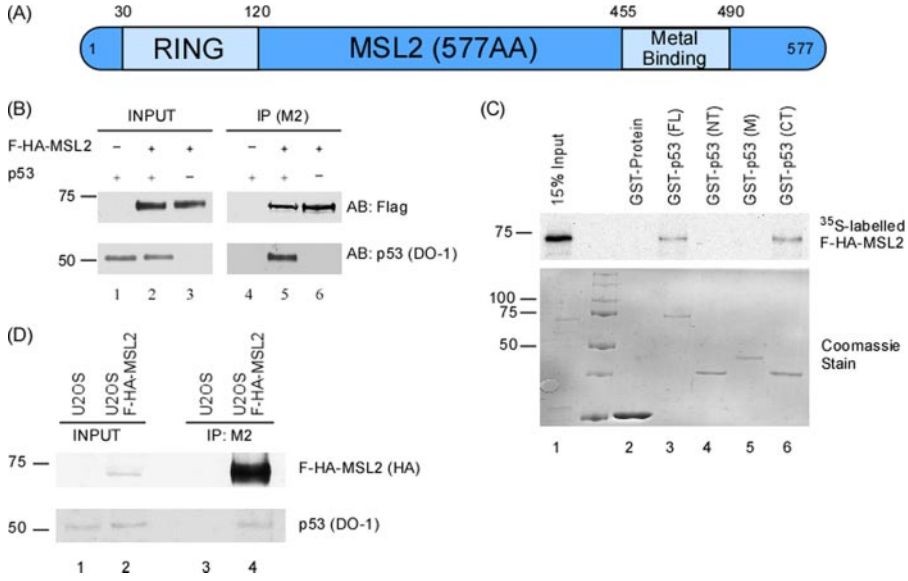

FIGURE 1. **MSL2, a novel interacting partner for p53.** *A*, schematic representation of MSL2, a 577-amino acid protein containing an N-terminal RING domain (residues 30–120) and a C-terminal metal binding domain (residues 455–490). *B*, co-immunoprecipitation of MSL2 and p53. H1299 cells were transfected with expression plasmids for F-HA-MSL2 and p53 as indicated. 24 h post-transfection, cells were lysed, and FLAG-tagged MSL2 was immunoprecipitated (*IP*) using M2-agarose beads. Bound proteins were eluted using FLAG-peptide. Inputs (*left panel*) and elutions (*right panel*) were analyzed by Western blot with the indicated antibodies. *C*, MSL2 interacts directly with the C-terminal region of p53 *in vitro* in a GST pulldown assay. The wild type GST-p53 full-length protein (GST-p53) (*lane 3*), the N terminus of p53 protein (residues 1–73) (*lane 4*), the middle part of p53 (residues 100–290) (*lane 5*), the C terminus of p53 (residues 290–393) (*lane 6*), or GST alone (*lane 2*) was used in a GST pulldown assay with *in vitro* translated ^{35}S-labeled full-length F-HA-MSL2. *D*, stably expressed F-HA-MSL2 immunoprecipitates endogenous p53. U2OS cells and a U2OS cell line that stably expresses F-HA-MSL2 were used for immunoprecipitations using M2-beads to capture FLAG-tagged proteins. Inputs and eluted precipitates were analyzed by Western blot as indicated.

midino-2-phenylindole in the last wash to visualize the nuclei. For the leptomycin B treatment, cells were incubated 24 post-transfection for 4 h with leptomycin B (Calbiochem) at a final concentration of 25 ng/ml before fixation. Quantitation of subcellular localization is based on 100 cells counted for each sample from three separate experiments. Subcellular localization was quantified for three separate experiments and presented as the mean ± S.D.

Preparation of Cytoplasmic and Nuclear Fractions—Cells were harvested, rinsed with phosphate-buffered saline, and pelleted. The cells were then suspended in 5 volumes of cold HB buffer (10 mM Tris, pH 7.9, 1.5 mM $MgCl_2$, 10 mM KCl, protease inhibitor mixture (Sigma)) and allowed to swell on ice for 15 min, after which Triton X-100 was added to a final concentration of 0.2%. After vortexing for 5 s, the homogenate was spun for 10 min at 1000 × *g*. The supernatant, containing the cytoplasmic fraction, was transferred to a fresh tube, and the salt concentration was adjusted to 200 mM with 5 M NaCl. The crude nuclear pellet was suspended in FLAG-lysis buffer and vortexed vigorously at 4 °C for 30 min. The homogenate was centrifuged for 15 min at 20,000 × *g*. Nuclear and cytoplasmic factions were analyzed by Western blot as indicated.

siRNA-mediated Knockdown of MSL2 and DNA Damage Treatment—The ablation of MSL2 was performed by transfection of U2OS cells with ON-TARGETplus SMARTpool oligoset by Dharmacon (Dharmacon L020828-01), consisting of four different oligos targeting four different regions of MSL2. Transfections of the siMSL1 or control siRNA (ON-TARGETplus siControl non-targeting pool D-001810-10-20 (Dharmacon)) was performed by using Lipofectamine 2000 according to the manufacturer's protocol (Invitrogen). To induce DNA damage, cells were treated with etoposide (20 μM) for 6 h.

RESULTS

MSL2 Is a Novel Binding Partner of p53—Human MSL2 is the homolog to the *Drosophila melanogaster* protein male-specific lethal-2, a member of the fruit fly dosage compensation complex (49–51). Human MSL2 is a 577-amino acid, 70-kDa protein that contains an N-terminal RING domain and a C-terminal metal-binding domain (Fig. 1*A*) (52). hMOF, another member of the mammalian MSL complex (49–51), has been shown to interact, modify, and regulate p53 (53), suggesting a potential regulatory node between the mammalian dosage compensation complex and p53. MSL2 is the only member of the mammalian dosage compensation complex containing a RING domain with potential E3 ligase function (49, 50), leading us to determine whether p53 interacts with this member of the complex in addition to the known interaction between p53 and hMOF (53). p53 null H1299 cells were transfected with expression plasmids for p53 and F-HA-MSL2, cells were harvested and lysed 24 h post-transfection, and tagged MSL2 was immunoprecipitated. Western blot analysis of inputs (Fig. 1*B*, *lanes 1–3*) and immunoprecipitates (Fig. 1*B*, *lanes 4–6*) shows that MSL2 immunoprecipitates co-expressed p53 *in vivo* (Fig. 1*B*, *lane 5*). An *in vitro* GST pulldown assay was used to determine whether the p53 interaction with MSL2 is direct and to map the specific p53 domain involved in the interaction (Fig. 1*C*). Recombinant full-length GST-p53 (Fig. 1*C*, *lane 3*), as well as a C-terminal GST-p53 fragment (Fig. 1*C*, *lane 6*), was able to interact with *in vitro* translated, ^{35}S-labeled F-HA-MSL2 *in vitro*. Neither GST-protein alone nor the GST-p53(NT) and GST-p53(M) subfragments were able to interact with MSL2 (Fig. 1*C*, *lanes 2, 4*, and *5*, respectively). Currently, no commercial antibodies are available that can detect human MSL2. To support the *in vivo* interaction data obtained from cotransfection experiments, a U2OS cell line was established that stably expresses low levels of F-HA-MSL2. Using U2OS wild type cells as controls together with the F-HA-MSL2 U2OS stable line, an interaction between endogenous p53 and the stably expressed F-HA-MSL2 was observed in co-immunoprecipitation experiments. Low levels of stably expressed F-HA-

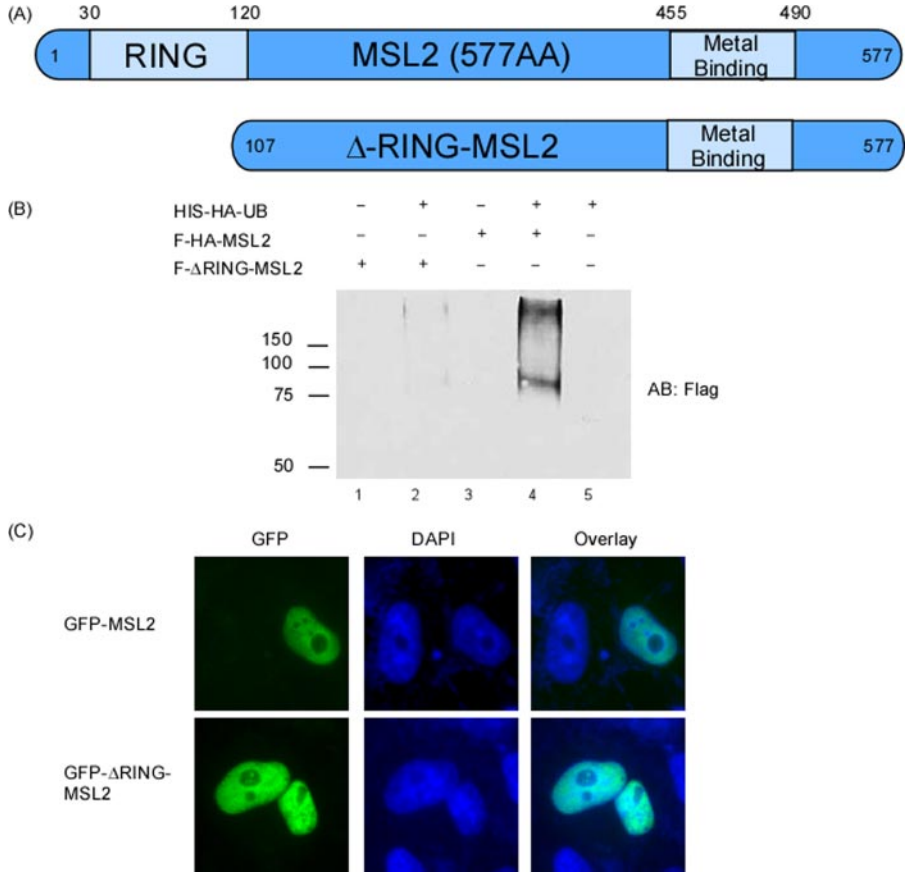

FIGURE 2. **Effect of the MSL2-RING domain on intrinsic E3 ligase activity and subcellular localization of MSL2.** *A*, schematic representation of full-length MSL2 and ΔRING-MSL2, a truncation mutant with the N-terminal 107 amino acids deleted to remove the active RING domain. *B*, MSL2 has ubiquitination activity. 293 cells were transfected with tagged wild type MSL2 and ΔRING-MSL2 constructs in the presence of His-HA-ubiquitin (*UB*). After treatment with the proteasome inhibitor MG132 for 4 h, cells were lysed and ubiquitinated proteins purified using Ni-NTA beads. Elutions were analyzed by Western blot as indicated. *AB*, antibody. *C*, MSL2 and ΔRING-MSL2 localize to the nucleus. H1299 cells were transfected with GFP-tagged full-length MSL2 and ΔRING-MSL2, and their subcellular localization was observed by fluorescent microscopy. *DAPI*, 4,6-diamidino-2-phenylindole.

MSL2 co-immunoprecipitate endogenous p53 from F-HA-U2OS cells (Fig. 1*D*, *lane 4*), whereas no p53 was detected after control immunoprecipitation from wild type U2OS cells (Fig. 1*D*, *lane 3*). Although the use of a stable line does not entirely substitute for co-immunoprecipitations of endogenous proteins, the observed interaction in the stable cell line supports the overexpression and *in vitro* interaction data presented in Fig. 1, *B* and *C*, respectively. Together, these experiments identify MSL2 as a novel interacting partner for p53 both *in vivo* and *in vitro*.

Effect of the MSL2-RING Domain on Intrinsic E3 Ligase Activity and Subcellular Localization of MSL2—Proteins containing a RING domain commonly possess intrinsic E3 ligase activity (54). To establish whether MSL2 has a functional RING domain capable of promoting ubiquitination, we generated a truncation mutant that has the RING domain deleted (ΔRING-MSL2) (Fig. 2*A*). To test whether MSL2 has intrinsic E3 ligase activity and whether this activity is dependent on the RING domain, a His_6-tagged ubiquitin construct was cotransfected with MSL2 or ΔRING-MSL2, and their ability to autoubiquitinate was analyzed. Ubiquitinated proteins were purified using Ni-NTA beads, and Western blot analysis of the elutions showed that wild type MSL2 (Fig. 2*B*, *lane 4*), but not ΔRING-MSL2 (Fig. 2*B*, *lane 2*), could autoubiquitinate. To ensure that the deletion of the RING domain does not affect the subcellular localization of MSL2, GFP-tagged full-length MSL2 and ΔRING-MSL2 were transfected into U2OS cells, and the localization of transfected MSL2 constructs was observed by fluorescent microscopy. As shown in Fig. 2*C*, full-length GFP-MSL2 (*upper panel*) and GFP-ΔRING-MSL2 (*lower panel*) localize to the nucleus when expressed exogenously, indicating that the MSL2-RING domain, although required for the ubiquitination activity of MSL2, does not affect the subcellular localization of MSL2.

MSL2 Is an E3 Ligase for p53—To determine whether MSL2 can act as an E3 ubiquitin ligase for p53, H1299 cells were transfected with p53 and either wild type MSL2 or ΔRING-MSL2 in the presence of His-tagged ubiquitin. After purification of ubiquitinated proteins, Western blot analysis showed that MSL2, but not ΔRING-MSL2, could ubiquitinate p53 *in vivo* (Fig. 3*A*, *lanes 3* and *5*, respectively). To ensure that the loss of p53 ubiquitination by the ΔRING-MSL2 construct was not due to a loss of interaction between p53 and the MSL2 constructs, H1299 cells were transfected with HA-tagged p53 alone (Fig. 3*B*, *lanes 1* and *6*) or in the presence of either FLAG-tagged full-length MSL2 (*lanes 2* and *7*) or FLAG-tagged ΔRING-MSL2 (*lanes 3* and *8*). As shown in Fig. 3*B*, *lanes 7* and *9*, respectively, both full-length MSL2 and ΔRING-MSL2 were able to co-immunoprecipitate HA-p53. Therefore, the loss of ubiquitination by ΔRING-MSL2 observed in Fig. 3*A*, *lane 5*, was caused by the absence of the MSL2-RING domain rather than a lost interaction between p53 and ΔRING-MSL2. With the exception of Mdm2-mediated p53 monoubiquitination, occurring at low Mdm2 levels (28), and E4F1 ubiquitination in the hinge region (38), p53 polyubiquitination is associated primarily with targeting p53 for proteasomal degradation. Cotransfection of the various p53-specific E3 ligases with p53 leads to significant reduction of p53 levels (4). To determine whether MSL2 affects p53 levels, H1299 cells were transfected with p53 alone (Fig. 3*C*, *lane 2*) and in combination with either wild type MSL2 or ΔRING-MSL2 (Fig. 3*C*, *lanes 3–5*). Neither overexpression of MSL2 (Fig. 3*C*, *lanes 3* and *4*) or of ΔRING-MSL2 (Fig. 3*C*, *lane 5*) affected p53 levels after cotransfection (Fig. 3*C*, *lane 2 versus lanes 3–5*), indicating that MSL2-medi-

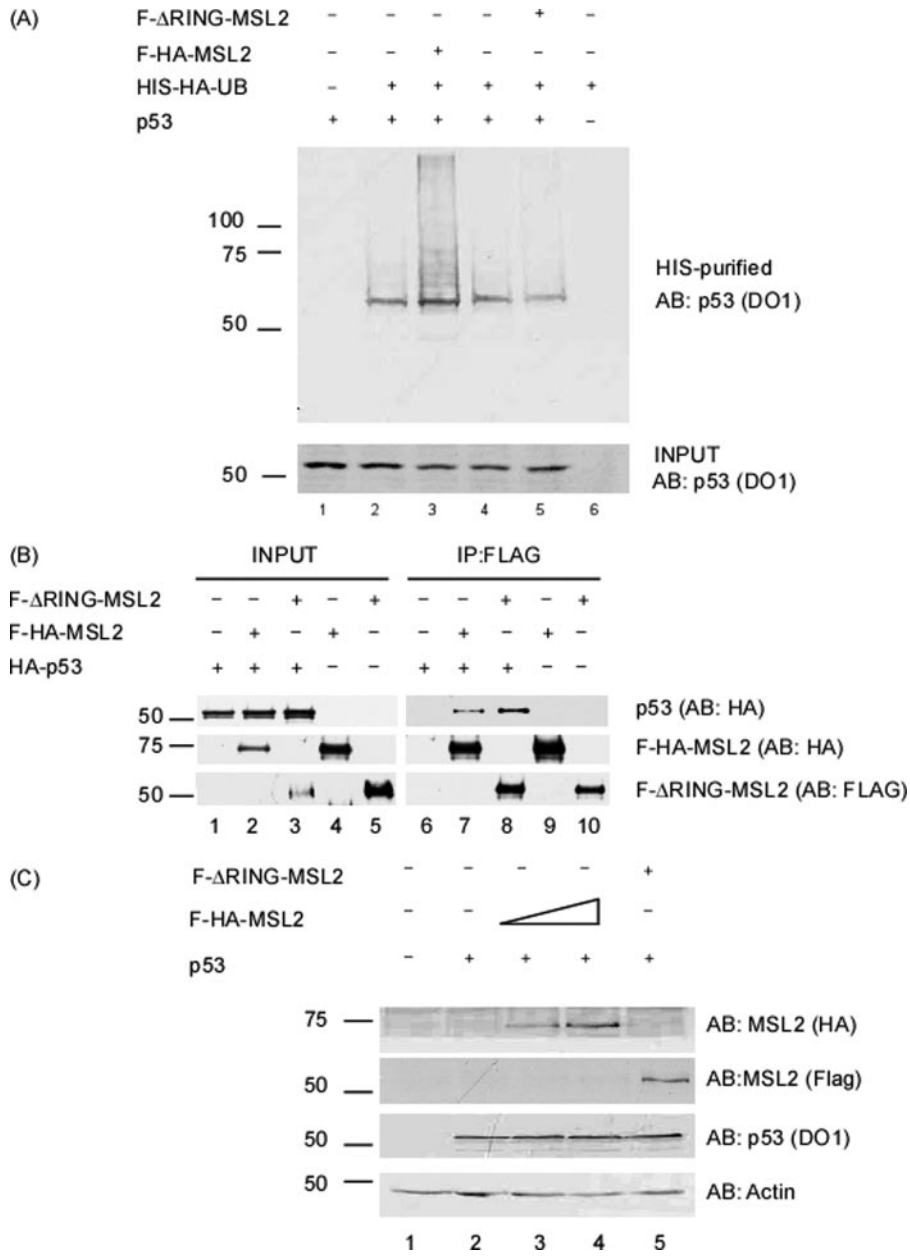

FIGURE 3. **MSL2 is an E3 ubiquitin ligase for p53 that does not regulate p53 levels.** *A*, MSL2 ubiquitinates p53. H1299 cells were transfected with p53, MSL2, ΔRING-MSL2, and His-HA-Ub as indicted. After MG132 treatment for 4 h, cells were lysed and ubiquitinated proteins purified using Ni-NTA beads. Inputs and eluates were analyzes by Western blot as indicated. *AB*, antibody. *B*, full-length MSL2 and ΔRING-MSL2 interact with p53. H1299 cells were cotransfected with HA-p53 in the presence or absence of FLAG-tagged expression constructs for full-length MSL2 or ΔRING-MSL2. Using M2-beads, FLAG-tagged MSL2 constructs were immunoprecipitated (*IP*), and elutions were analyzed for co-immunoprecipitation of HA-p53 by Western blot as indicated. *C*, MSL2 expression does not affect p53 levels. H1299 cells were transfected with p53 in combination with either wild type or ΔRING truncation constructs of MSL2. Whole cell lysates were analyzed by Western blot as indicated.

somal control of p53 stability. In addition to targeting proteins for degradation, ubiquitination has been described as a signal for various degradation-independent events such as endocytosis, virus budding, changes in subcellular localization, and transcriptional regulation (55, 56). Because the majority of degradation-independent functions of ubiquitin affect the targets subcellular localization, the subcellular localization of p53 in the presence of MSL2 or ΔRING-MSL2 was analyzed (Fig. 4*A*). H1299 cells were transfected with p53 either alone (Fig. 4*A*, *panel I*), together with MSL2 (*II*), or ΔRING-MSL2 (*III*), and the localization of p53 was determined by immunofluorescent staining. When p53 was transfected alone (Fig. 4*A*, *panel I*) or in the presence of ΔRING-MSL2 (*III*), 85 and 86% of the transfected cells showed nuclear staining respectively (Fig. 4*B*). However, when p53 was cotransfected with MSL2 (Fig. 4*A*, *panel III*), only 54% of the transfected cells showed nuclear staining, whereas 46% showed cytoplasmic staining (Fig. 4*B*). This marked increase in cytoplasmic staining was dependent on the nuclear export machinery, as treatment with leptomycin B prevented the change in subcellular localization (Fig. 4*A*, *panel IV*, 83% nuclear staining). The observed change in subcellular localization was supported by fractionation experiments showing an increase in cytoplasmic p53 levels upon MSL2 cotransfection, whereas ΔRING-MSL2 did not promote such a change (Fig. 4*C*). Treatment with leptomycin B again confirms in fractionation experiments that the nuclear export machinery is required for MSL2-mediated p53 export (Fig. 4*D*). Together, these data show that MSL2-mediated ubiquitination promotes cytoplasmic localization of p53 that is dependent on the nuclear export machinery.

ated ubiquitination does not result in proteasomal degradation of p53 and hence does not regulate p53 stability *in vivo*.

MSL2-mediated Ubiquitination of p53 Promotes Cytoplasmic Localization of p53—At low levels, Mdm2-mediated p53 monoubiquitination promotes cytoplasmic localization of p53, whereas high Mdm2 levels target p53 for proteasomal degradation (28). Cotransfection of MSL2 in excess of p53 did not affect p53 levels (Fig. 3*C*), suggesting that MSL2-mediated p53 ubiquitination has functional consequences independent of proteasomal control of p53 stability. In addition to targeting proteins for degradation, ubiquitination has been described as a signal for various degradation-independent events such as endocytosis, virus budding, changes in subcellular localization, and transcriptional regulation (55, 56). Because the majority of degradation-independent functions of ubiquitin affect the targets subcellular localization, the subcellular localization of p53 in the presence of MSL2 or ΔRING-MSL2 was analyzed (Fig. 4*A*). H1299 cells were transfected with p53 either alone (Fig. 4*A*, *panel I*), together with MSL2 (*II*), or ΔRING-MSL2 (*III*), and the localization of p53 was determined by immunofluorescent staining. When p53 was transfected alone (Fig. 4*A*, *panel I*) or in the presence of ΔRING-MSL2 (*III*), 85 and 86% of the transfected cells showed nuclear staining respectively (Fig. 4*B*). However, when p53 was cotransfected with MSL2 (Fig. 4*A*, *panel III*), only 54% of the transfected cells showed nuclear staining, whereas 46% showed cytoplasmic staining (Fig. 4*B*). This marked increase in cytoplasmic staining was dependent on the nuclear export machinery, as treatment with leptomycin B prevented the change in subcellular localization (Fig. 4*A*, *panel IV*, 83% nuclear staining). The observed change in subcellular localization was supported by fractionation experiments showing an increase in cytoplasmic p53 levels upon MSL2 cotransfection, whereas ΔRING-MSL2 did not promote such a change (Fig. 4*C*). Treatment with leptomycin B again confirms in fractionation experiments that the nuclear export machinery is required for MSL2-mediated p53 export (Fig. 4*D*). Together, these data show that MSL2-mediated ubiquitination promotes cytoplasmic localization of p53 that is dependent on the nuclear export machinery.

MSL2 Ubiquitinates p53 at Two Novel Ubiquitination Sites, Lys-351 and Lys-357, Instead of the Canonical Six C-terminal Lysines Ubiquitinated by Mdm2

The major sites of Mdm2-mediated ubiquitination of p53 are located in the C-terminal transactivation domain (4); these six

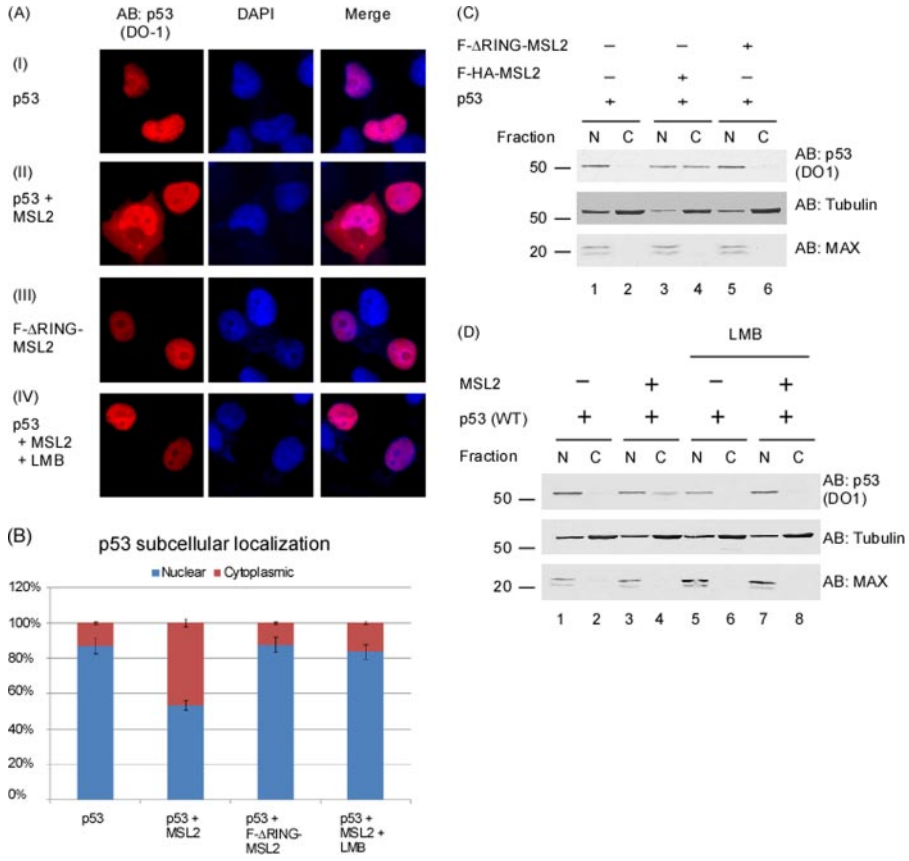

FIGURE 4. **MSL2-mediated ubiquitination of p53 promotes cytoplasmic localization of p53.** *A*, MSL2-mediated p53 ubiquitination promotes p53 cytoplasmic localization. H1299 cells were transfected with p53 alone (*I*) or in combination with wild type (*II*) or truncated MSL2 (*III*). Treatment with leptomycin B for 4 h prior to fixation inhibited MSL2-mediated cytoplasmic localization of p53 (*IV*). Cells were stained using antibodies for p53 as indicated and counterstained with 4,6-diamidino-2-phenylindole (*DAPI*). *B*, quantitation of subcellular localization shown in Fig. 3*A*. Subcellular localization was quantified for three separate experiments and presented as the mean ± S.D. *C*, fractionation of H1299 cells transfected with p53 alone or in combination with wild type MSL2 or ΔRING-MSL2. Cells were fractionated and analyzed by Western blot as indicted. *AB*, antibody. *D*, fractionation of control or leptomycin B-treated H1299 cells transfected with p53 alone or in combination with MSL2. Nuclear (*N*) and cytoplasmic (*C*) fractions were analyzed by Western blot as indicated.

C-terminal lysines are shown to be required for Mdm2-mediated cytoplasmic localization of p53 (27, 28, 31). Additionally, more recent studies have shown that these lysines contribute to p53 cytoplasmic localization not only because they act as acceptor sites for ubiquitination but also because ubiquitination at these sites results in the exposure of a C-terminal nuclear export signal and promotes dissociation from Mdm2 (30). To map the sites of MSL2-dependent ubiquitination, p53–6KR and p53–8KR (6KR + K351R/K357R) mutant constructs with the six or eight C-terminal lysines mutated to arginine, respectively, were analyzed (Fig. 5*A*). To map the ubiquitination sites used by MSL2 and to compare the location of these lysines to those utilized by Mdm2, H1299 cells were transected with the different p53 constructs and His-tagged ubiquitin either alone or in combination with Mdm2 or MSL2 (Fig. 5*B*). Although Mdm2-mediated ubiquitination of p53–6KR was significantly reduced (Fig. 5*B*, *lane 3 versus lane 6*), MSL2-mediated ubiquitination levels were comparable between p53 and p53–6KR (*lane 2 versus lane 5*). However, MSL2-mediated ubiquitination was completely abrogated when the p53–8KR mutant construct was used (Fig. 5*B*, *lane 8*), whereas ubiquitination levels of p53–6KR and p53–8KR by Mdm2 were similar (*lane 6 versus lane 9*). Furthermore, a p53 construct that contains lysine to arginine mutations only at positions Lys-351 and Lys-357 could not be ubiquitinated by MSL2 *in vivo* (Fig. 5*C*, *lane 3 versus lane 7*), whereas Mdm2 was able to promote ubiquitination of $p53^{K351R/K357R}$. These data suggests that Lys-351 and Lys-357 are required for MSL2-mediated ubiquitination of p53. As the C-terminal region of p53 had been shown to mediate the interaction between p53 and MSL2, mutation of lysines within this region could inhibit this interaction, potentially causing the observed loss of MSL2-mediated ubiquitination of the $p53^{K351R/K357R}$ mutant. To test whether $p53^{K351R/K357R}$ is still able to interact with MSL2, FLAG-tagged p53 and $p53^{K351R/K357R}$ were cotransfected with GFP-MSL2, and their interaction was assayed by co-immunoprecipitation. As shown in Fig. 5*D*, both FLAG-p53 and FLAG-$p53^{K351R/K357R}$ were able to co-immunoprecipitate GFP-MSL2 (Fig. 5*D*, *lanes 7* and *9*, respectively), indicating that these lysines are indeed ubiquitination sites for MSL2 and that loss of $p53^{K351R/K357R}$ ubiquitination by MSL2 is not due to a reduced interaction between the mutant p53 and MSL2. Together these *in vivo* data suggest that MSL2 ubiquitination of p53 targets the residues Lys-351 and Lys-357 instead of the six C-terminal lysines primarily targeted by Mdm2.

MSL2-mediated Ubiquitination at Lys-351 and Lys-357 Is Required for p53 Cytoplasmic Localization—Establishing cytoplasmic pools of p53 is thought to rely predominantly on p53 monoubiquitination of the C-terminal lysines by Mdm2. Although Mdm2-mediated cytoplasmic localization of p53 requires the availability of the six C-terminal lysines (27, 57–59), the ubiquitination site mapping presented in Fig. 5 suggests that MSL2-mediated cytoplasmic localization requires Lys-351 and Lys-357. Therefore, if MSL2-mediated ubiquitination of p53 is required for the cytoplasmic localization of p53 shown in Fig. 4, MSL2 would be expected to promote cytoplasmic localization of p53–6KR, whereas the subcellular localization of p53–8KR or $p53^{K351R/K357R}$ should not be affected. In contrast, Mdm2-mediated ubiquitination should promote cytoplasmic localization of $p53^{K351R/K357R}$, whereas neither p53–6KR nor p53–8KR should be affected. To test this differential regulation of the various p53 mutants, H1299 cells were transfected with the indicated p53 mutants constructs alone or in combination with MSL2 or Mdm2 (Fig. 6). A comparison of

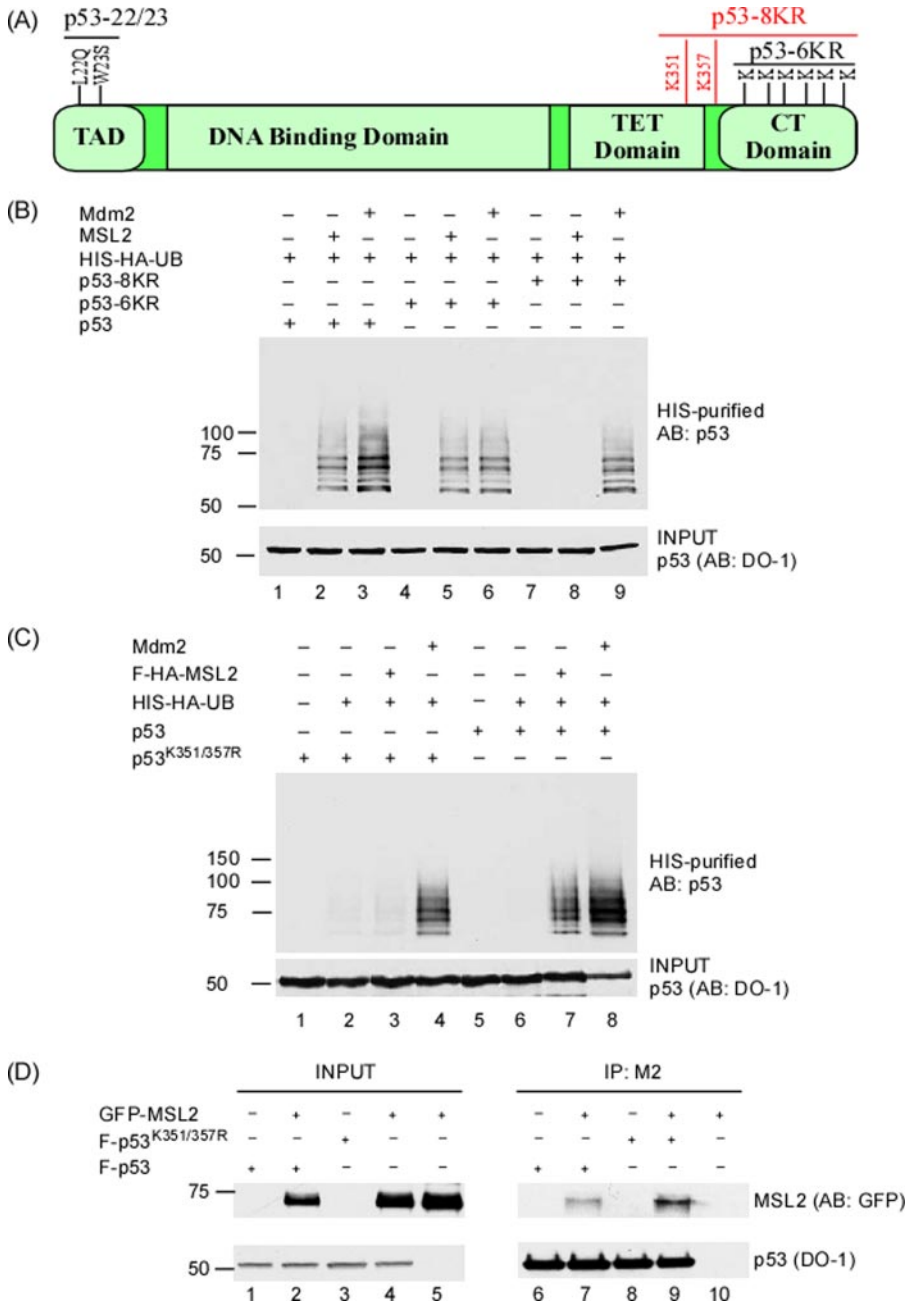

FIGURE 5. **Mapping the site of MSL2-mediated p53 ubiquitination.** *A*, schematic representation of p53 domain structure (transactivation domain (*TAD*) 1–42; DNA-binding domain 100–300; tetramerization (*TET*) domain 300–355; C-terminal transactivation (*CT*) domain 363–393) and location of amino acid mutations introduced in p53 expression constructs that were analyzed in ubiquitination and localization experiments. *B*, mapping of the site of MSL2-mediated ubiquitination of p53. H1299 cells were transfected with wild type p53, p53–6KR, or p53–8KR (6KR + K351/K357R) and His-HA-Ub alone or together with either MSL2 or Mdm2 as indicated. Ubiquitinated p53 was purified using Ni-NTA beads after MG132 treatment for 4 h, and inputs and precipitates were analyzed by Western blot as indicated. *AB*, antibody. *C*, mutation of p53 lysines K351R/K357R prevents MSL2-mediated ubiquitination. H1299 cells were transfected with wild type or mutant p53 and His-HA-Ub, MSL2, and Mdm2 as indicated. Inputs and Ni-NTA-purified immunoprecipitates (*IP*) were analyzed by Western blot as indicated. *D*, co-immunoprecipitation of GFP-MSL2 by wild type p53 and $p53^{K351R/K357R}$. H1299 cells were cotransfected with GFP-MSL2 and FLAG-tagged wild type and mutant p53 constructs. FLAG-tagged p53 constructs were immunoprecipitated using M2-beads, and eluates were analyzed by Western blot as indicated.

p53–6KR localization alone, in combination with MSL2, or in combination with Mdm2 (Fig. 6*A*, *I—III*, respectively) shows that unlike Mdm2, MSL2 retains the ability to promote cytoplasmic localization of p53–6KR. Although only 17% of the transfected cells showed cytoplasmic staining for p53–6KR in the presence of Mdm2 (compared with 15% when p53–6KR was transfected alone), cotransfection of p53–6KR in combination with MSL2 resulted in cytoplasmic localization of p53–6KR in 46% of the transfected cells (Fig. 6*B*, *bars 1–3*). However, this effect was lost when p53–8KR was used, as p53–8KR cannot be ubiquitinated by MSL2 (Fig. 6, *A*, *panels IV–VI*, and *B*, *bars 4–6*). Although also unable to promote cytoplasmic localization of p53–8KR (Fig. 6, *A*, *panel VI*, and *B*, *bar 6*), Mdm2 was able to induce cytoplasmic localization of $p53^{K351R/K357R}$ in 36% of the stained cells (Fig. 6, *A*, *panel IX*, and *B*, *bar 9*). However, MSL2 was unable to promote cytoplasmic localization of $p53^{K351R/K357R}$ as expected from the ubiquitination experiments (Fig. 6, *A*, *panel VIII*, and *B*, *bar 8*). Together, these data show that Mdm2 and MSL2 are both able to promote ubiquitin-mediated cytoplasmic localization of p53 by targeting different sets of lysines and that ubiquitination is required for such changes in p53 subcellular localization.

The MSL2 Interaction with p53 Is Required for MSL2-mediated Ubiquitination of p53 and the Resulting Change in Subcellular Localization

The data presented for the experiments using the ΔRING-MSL2 mutant (Figs. 2 and 4) and the $p53^{K351R/K357R}$ mutant (Figs. 5 and 6) indicate that MSL2-mediated ubiquitination of p53 is required for its ability to promote cytoplasmic localization of p53. However, to provide further evidence that MSL2-mediated ubiquitination of p53 is direct and that the interaction between p53 and MSL2 is required for p53 ubiquitination and changes in subcellular localization, the effects of additional MSL2 truncation mutants on p53 ubiquitination and subcellular localization were tested (Fig. 7). As shown in Figs. 2*C* and 3*B*, the ΔRING-MSL2 mutant was still able to localize to the nucleus and interact with p53, indicating that other regions of MSL2 are required

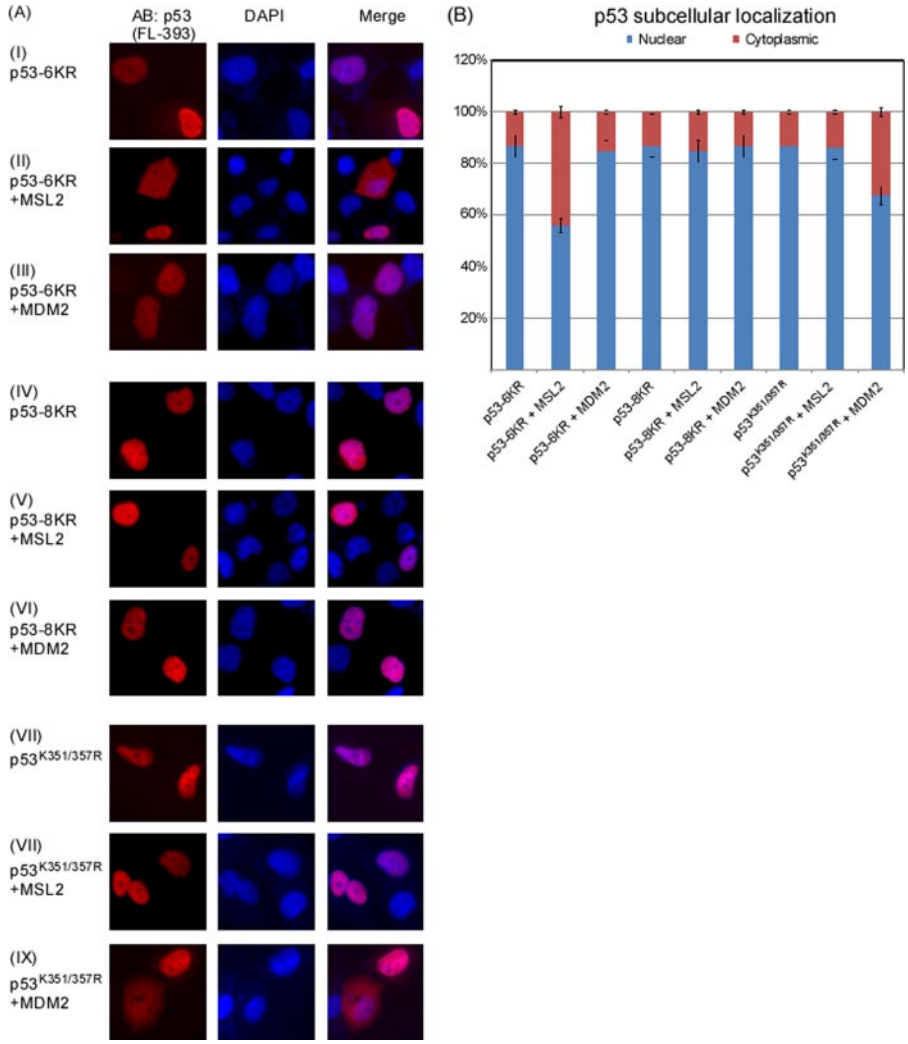

FIGURE 6. **MSL2 ubiquitination of p53 is required for p53 cytoplasmic localization.** *A*, analysis of MSL2-mediated cytoplasmic p53 localization of p53 mutants. H1299 cells were transfected with the p53 mutants alone or in combination with MSL2 or Mdm2 as indicated, and subcellular localization of p53 was detected by fluorescent microscopy after immunostaining. *AB*, antibody; *DAPI*, 4,6-diamidino-2-phenylindole. *B*, quantitation of subcellular localization of p53 mutants as determined by immunostaining. Values shown represent the average value obtained from three separate experiments. Subcellular localization was quantified for three separate experiments and presented as the mean ± S.D.

for MSL2-p53 interaction. Therefore, C-terminal MSL2 truncation mutants were generated (Fig. 7*A*), and their subcellular localization was analyzed. As shown in Fig. 7*B*, although full-length GFP-MSL2 and GFP-MSL2-(1–400) localized to the nucleus (*upper* and *lower panels*), the shorter GFP-MSL2-(1–200) showed a diffuse staining throughout the cell (*middle panel*). To determine whether the direct interaction between p53 and the MSL2 constructs is required for *in vivo* ubiquitination of p53, the interaction of the individual MSL2 constructs with p53 was tested by co-immunoprecipitation. FLAG-tagged p53 was cotransfected with the three GFP-MSL2 constructs, and tagged p53 was able to co-immunoprecipitate both full-length GFP-MSL2 and GFP-MSL2-(1–400) (Fig. 7*C*, *lanes 7* and *8*) while being unable to co-immunoprecipitate significant GFP-MSL2-(1–200) amounts detectable by Western blot (Fig. 7*C*, *lane 6*). These data, in combination with the co-immunoprecipitation data for the ΔRING-MSL2 constructs (Fig. 3*B*), suggest that the middle region of MSL2 is required for the interaction between MSL2 and p53. To test whether this direct interaction between MSL2 and p53 is required for p53 ubiquitination and the observed changes in subcellular localization, we tested the ability of the different MSL2 constructs to ubiquitinated p53 *in vivo*. As shown in Fig. 7*D*, full-length MSL2 and MSL2-(1–400) were able to induce p53 ubiquitination (Fig. 7*D*, *lanes 3* and *4*), while MSL2–1-200 lost almost all ubiquitination activity (Fig. 7*D*, *lane 5*), suggesting that binding of MSL2 to p53 is required for MSL2-mediated p53 ubiquitination. To provide additional proof that the interaction and resulting ubiquitination are required for MSL2-mediated effects on p53 localization, the effects of the different GFP-MSL2 constructs on p53 subcellular localization were tested. As shown in Fig. 7*E*, GFP-MSL2 and GFP-MSL2-(1–400) were able to promote cytoplasmic localization of p53 in an average of 37 and 35% of transfected cells (Fig. 7, *E*, *panels II* and *III*, and *F*, *bars 2* and *3*), whereas GFP-MSL2-(1–200), which is unable to bind and ubiquitinate p53, did not affect p53 localization (Fig. 7, *E*, *panel IV*, and *F*, *bar 4*). These results from immunostaining experiments were confirmed by fractionation experiments after cotransfection of p53 with the MSL2 constructs (Fig. 7*G*). Cotransfection of p53 with full-length GFP-MSL2 and GFP-MSL2-(1–400) led to increased p53 levels detected in cytoplasmic fractions (Fig. 7*G*, *lanes 4* and *8*), whereas cotransfection with GFP-MSL2-(1–200) had no effect on the levels of cytoplasmic p53 detected after fractionation (Fig. 7*G*, *lane 6*). Together, the studies using MSL2 truncation mutants provide additional proof that the interaction between MSL2 and p53 is required for MSL2-mediated ubiquitination and the resulting changes in p53 subcellular localization. However, in addition to the interaction between the two proteins, ubiquitination of p53 is required for the changes in subcellular localization, as the loss of ubiquitination prevents changes in subcellular localization regardless of the interaction, as shown by studies using the ΔRING-MSL2 construct or $p53^{K351R/K357R}$.

Unlike Mdm2, MSL2 Is Able to Promote Ubiquitination and Cytoplasmic Localization of $p53^{QS}$—As is the case for p53–6KR, $p53^{Q22/23S}$ ($p53^{QS}$), a well established p53 mutant that lost its ability to interact with Mdm2 due to mutation in the N-terminal Mdm2 binding site (43), should not be able to form

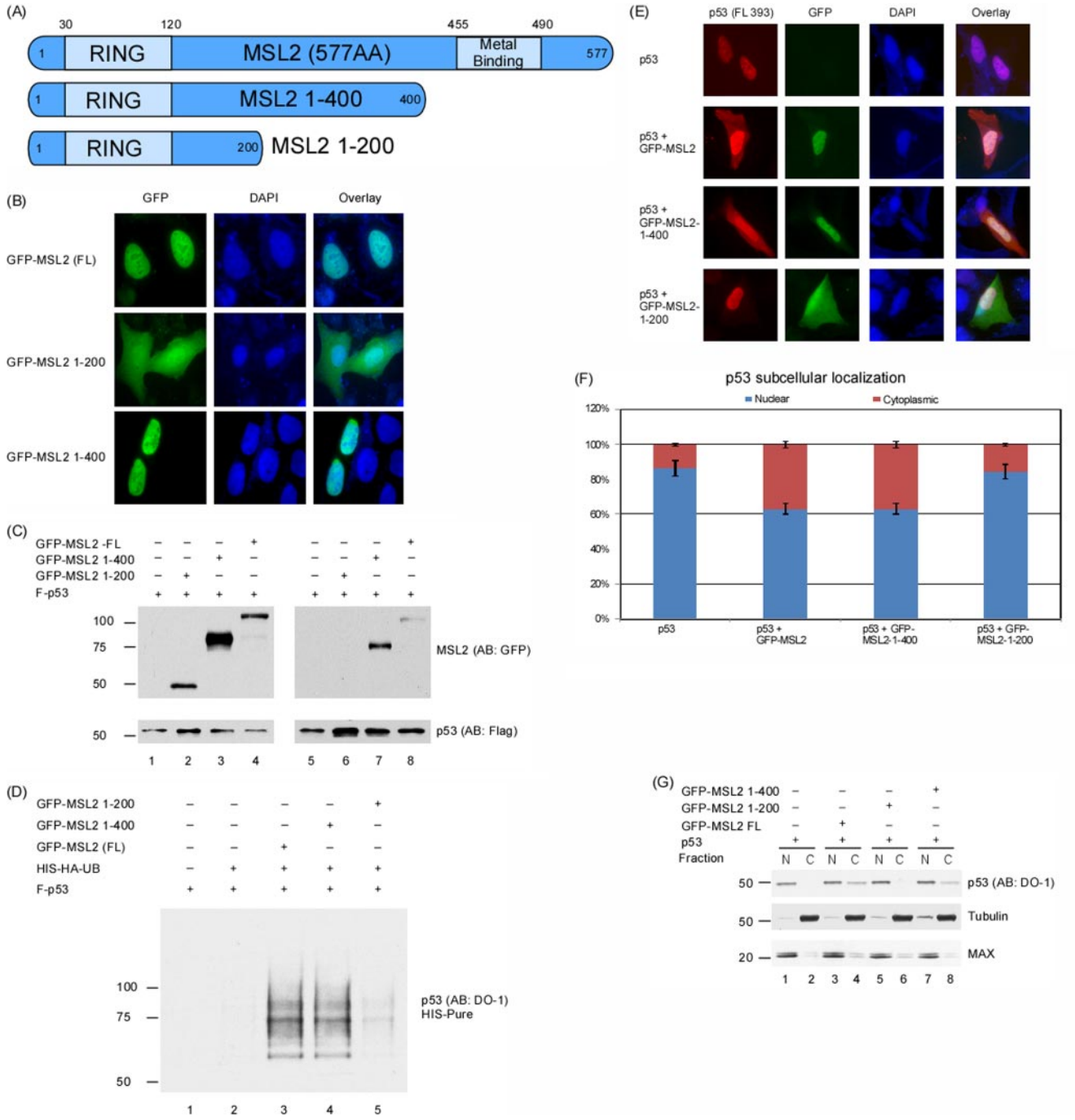

FIGURE 7. **MSL2-mediated ubiquitination and changes in subcellular localization require the MSL2-p53 interaction.** *A*, schematic representation of GFP-tagged MSL2 truncation constructs used in the interaction, localization and ubiquitination experiments. *B*, subcellular localization of the GFP-MSL2 truncation constructs. U2OS cells were transfected with the different GFP-MSL2 constructs and their subcellular localization was analyzed by fluorescent microscopy. *DAPI*, 4,6-diamidino-2-phenylindole. *C*, interaction of F-p53 with GFP-MSL2 truncation constructs *in vivo*. H1299 cells were transfected with F-p53 alone or in combination with the different GFP-tagged MSL2 truncation constructs. After M2 immunoprecipitation, inputs and eluates were analyzed by Western blot as indicated. *AB*, antibody. *D*, ubiquitination of p53 by GFP-MSL2 constructs *in vivo*. H1299 cells were transfected with wild type p53 alone or in combination with His-HA-Ub and the GFP-MSL2 truncation constructs as indicated. Ubiquitinated p53 was purified using Ni-NTA beads after MG132 treatment, and precipitates were analyzed by Western blot as indicated. *E*, effect of GFP-MSL2 truncation constructs on p53 subcellular localization. U2OS cells were transfected with p53 alone or in combination with the various GFP constructs as indicated. Subcellular localization of p53 and GFP-MSL2 was detected by fluorescent microscopy. *F*, quantitation of subcellular localization of p53 after cotransfection with GFP-MSL2 constructs as determined by immunostaining. Values shown represent the average value obtained from three separate experiments. Subcellular localization was quantified for three separate experiments and presented as the mean ± S.D. *G*, effect of GFP-MSL2 constructs on p53 subcellular localization determined by fractionation. H1299 cells were transected with p53 alone or in combination with the different GFP-MSL2 constructs as indicated. After fractionation, samples were analyzes by Western blot as indicated. *N*, nuclear fraction; *C*, cytoplasmic fraction.

Mdm2-mediated ubiquitination-dependent cytoplasmic pools. Although $p53^{QS}$ was found in the nucleus in the majority of MEF cells derived from $p53^{QS}$ mutant mice, significant cytoplasmic staining was also reported (43). To provide further evidence that MSL2-mediated p53 ubiquitination affects p53 localization independent of Mdm2, we tested whether MSL2

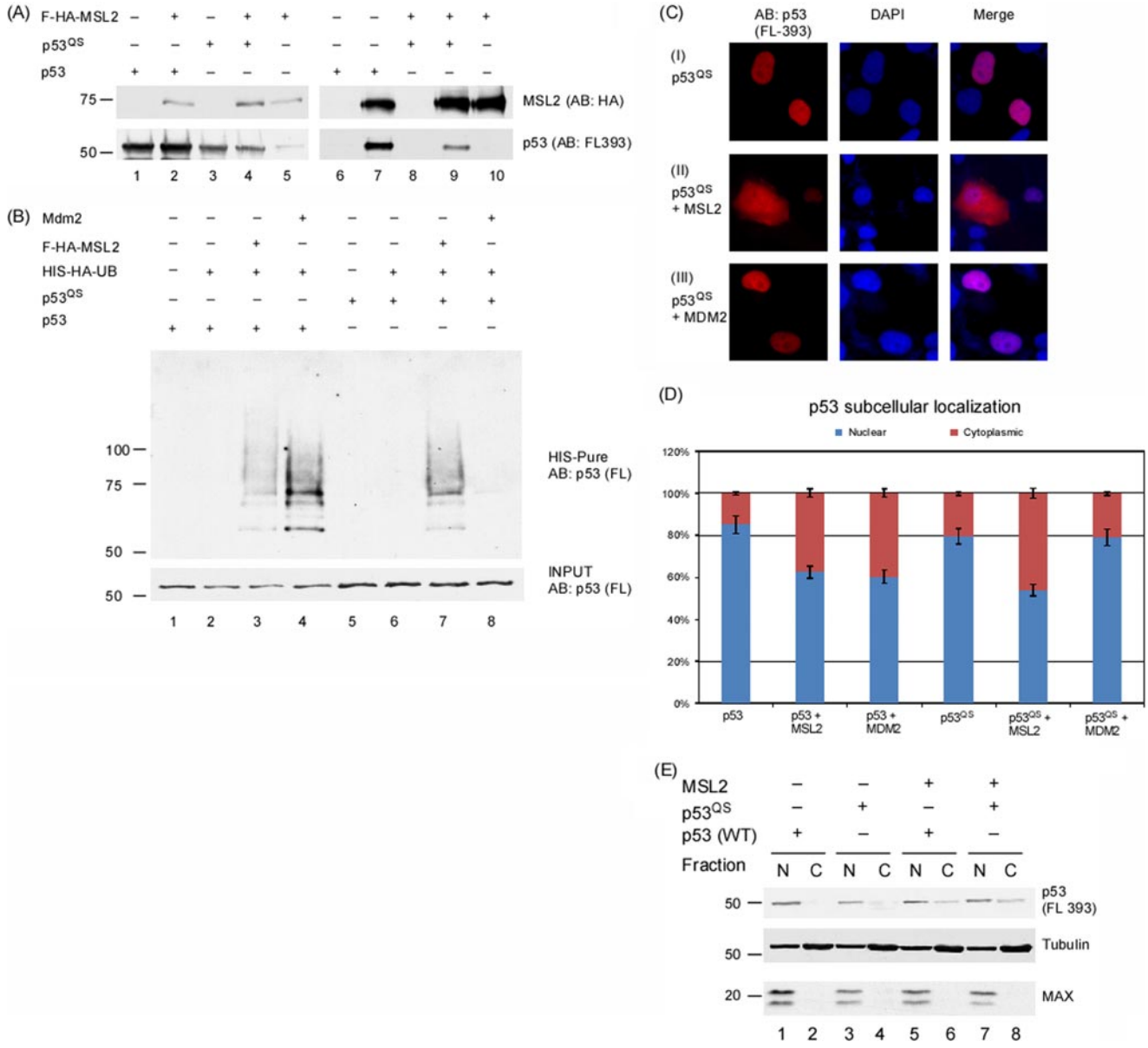

FIGURE 8. **Regulation of p53 by MSL2 is Mdm2-independent.** The effect of MSL2 on p53^{QS} is shown. *A*, co-immunoprecipitation of wild type and mutant p53 by F-HA-MSL2. 293 cells were cotransfected as indicated, and FLAG-tagged MSL2 was immunoprecipitated using M2-beads. Eluates were analyzed by Western blot as indicated. *AB*, antibody. *B*, MSL2, but not Mdm2, ubiquitinates p53^{QS} *in vivo*. H1299 cells were transfected with wild type or mutant p53 alone or in combination with His-HA-Ub and either Mdm2 or MSL2 constructs as indicated. Ubiquitinated p53 was purified using Ni-NTA beads after MG132 treatment, and precipitates were analyzed by Western blot as indicated. *C*, effect of MSL2 or Mdm2 on p53^{QS} subcellular localization. H1299 cells were transfected with p53^{QS} alone or in combination with MSL2 and Mdm2 as indicated. Subcellular localization of p53 was analyzed by fluorescent microscopy after immunostaining for p53. *D*, quantitation of subcellular localization of p53 wt and p53^{QS} after cotransfection with MSL2 or MDM2 as determined by immunostaining. Values shown represent the average value obtained from three separate experiments. Subcellular localization was quantified for three separate experiments and presented as the mean ± S.D. *E*, effect of MSL2 or Mdm2 constructs on p53 wild type and mutant subcellular localization determined by fractionation. H1299 cells were transected with wild type or mutant p53 alone or in combination with MSL2 as indicated. After fractionation, samples were analyzed by Western blot as indicated. *N*, nuclear fraction; *C*, cytoplasmic fraction.

could regulate the cytoplasmic localization of p53^{QS} (Fig. 8). As demonstrated above, MSL2 needs to interact with p53 in order to promote its ubiquitination and cytoplasmic localization. To test the interaction between MSL2 and p53^{QS}, tagged MSL2 was cotransfected with wild type p53 or p53^{QS}, and their interaction was analyzed by co-immunoprecipitation. MSL2 was able to co-immunoprecipitate both wild type p53 (Fig. 8*A*, *lane 7*) and p53^{QS} (Fig. 8*A*, *lane 9*), demonstrating that MSL2 and p53^{QS} are able to interact *in vivo*. Ubiquitination assays show that although both Mdm2 and MSL2 are able to ubiquitinate wild type p53 (Fig. 8*B*, *lanes 3* and *4*), only MSL2 is able to ubiquitinate p53^{QS} (Fig. 8*B*, *lane 7*). As expected, analogous to the observed increase in cytoplasmic localization for p53–6KR, MSL2 promotes cytoplasmic localization of p53^{QS} in 46% of cotransfected cells, whereas Mdm2 loses its ability to promote cytoplasmic localization of this mutant (Fig. 8, *C*, *panels II* and *III*, and *D* (bars 5 and 6); staining for wild type p53 is not shown, see Fig. 4A for representative staining). Changes in subcellular localization of p53^{QS} when cotransfected with MSL2 were confirmed by fractionation experiments (Fig. 8*E*). MSL2 cotrans-

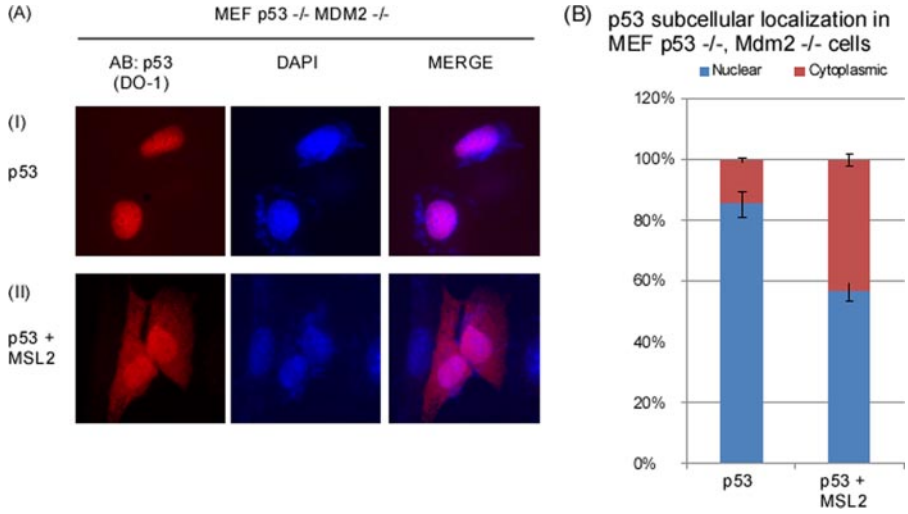

FIGURE 9. **Changes in MSL2-mediated p53 subcellular localization are Mdm2-independent.** *A*, MSL2 can promote cytoplasmic localization of p53 in MEF $p53^{-/-}$,$Mdm2^{-/-}$ cells. Mdm2/p53 double null MEF cells were transfected and stained for p53 localization as indicated. *DAPI*, 4,6-diamidino-2-phenylindole. *B*, quantitation of subcellular localization of p53 alone or in combination with MSL2 in MEF $p53^{-/-}$, $Mdm2^{-/-}$ cell lines. Values shown represent the average value obtained from three separate experiments. Subcellular localization was quantified for three separate experiments and presented as the mean ± S.D.

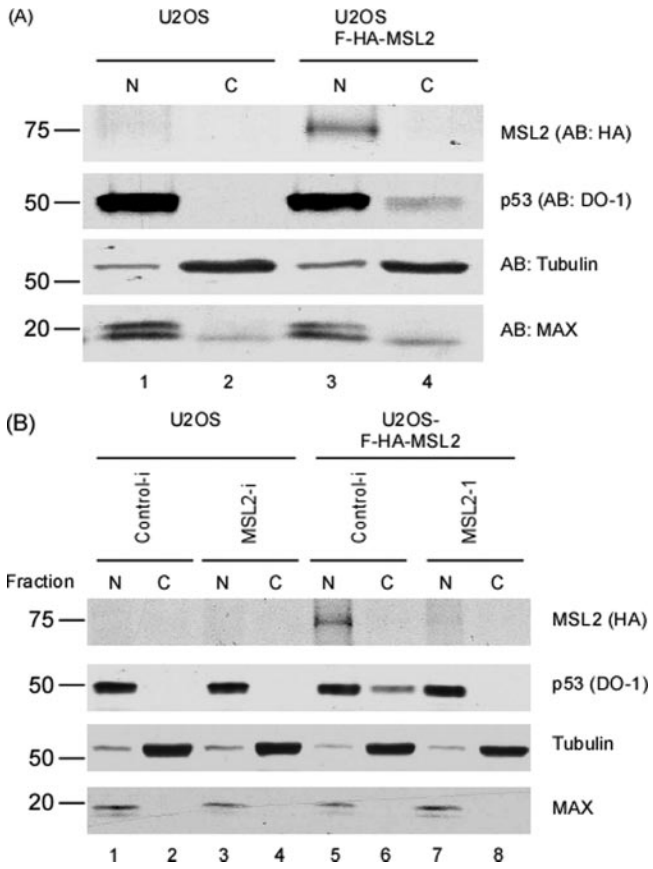

FIGURE 10. **Effect of MSL2 on endogenous p53 subcellular localization in U2OS parental compared with U2OS-F-HA-MSL2 stable line.** *A*, subcellular localization of endogenous p53 in U2OS parental and U2OS-F-HA-MSL2 stable line. Parental U2OS cells and U2OS cells stably expressing F-HA-MSL2 were fractionated to obtain nuclear (*N*) and cytoplasmic (*C*) fractions, and these were analyzed by Western blot as indicated. *AB*, antibody. *B*, effect of siRNA-mediated knockdown of MSL2 on p53 subcellular localization. Parental U2OS and U2OS-F-HA-MSL2 stable line were transfected with control siRNA oligos or oligos specific for MSL2 knockdown. After three rounds of transfection, cells were fractionated to obtain nuclear and cytoplasmic extracts, and fractions were analyzed by Western blot as indicated.

fection resulted in a marked increase in wild type p53 and $p53^{QS}$ in the cytoplasmic fraction (Fig. 8*E*, *lanes 6* and *8* compared with *lanes 2* and *4*). In summary, unlike Mdm2, MSL2 is able to interact with $p53^{QS}$, promote its ubiquitination, and increase cytoplasmic levels of $p53^{QS}$.

MSL2-mediated Cytoplasmic Localization of p53 Is Mdm2-independent—To further establish that changes in p53 subcellular localization were entirely specific to MSL2 and not from any nonspecific effects of Mdm2, we used a MEF $p53^{-/-}$ $Mdm2^{-/-}$ cell line for cotransfection assays with p53 and MSL2 (Fig. 9). As in the case of H1299 cells described earlier, transfection of p53 alone into MEF $p53^{-/-}$ $Mdm2^{-/-}$ cells resulted in cytoplasmic localization of p53 in only 16% of the transfected cells (Fig. 9, *A*, *panel I*, and *B*, *bar 1*), whereas cotransfection with MSL2 resulted in 43% of the cells with cytoplasmic p53 localization (Fig. 9, *A*, *panel II*, and *B*, *bar 2*). Together with its ability to promote cytoplasmic localization of the p53–6KR and the $p53^{QS}$ mutants, which could not be shuttled to the cytoplasm by Mdm2, these data from $Mdm2^{-/-}$ cells demonstrate that MSL2-mediated cytoplasmic localization of p53 is Mdm2-independent.

Stable Expression of F-HA-MSL2 Promotes Increased Cytoplasmic Localization of Endogenous p53 in U2OS Cells—The majority of p53 is commonly localized in the nucleus. To address whether MSL2 has an effect on the localization of endogenous p53, fractionation experiments were carried out in U2OS parental wild type cells and U2OS cells that stably express low levels of F-HA-MSL2. As shown in Fig. 10*A*, although virtually no endogenous p53 was detected in parental U2OS cells (Fig. 10*A*, *lanes 1* and *2*), cytoplasmic p53 was detected in U2OS cells that stably express F-HA-MSL2 (Fig. 10*A*, *lanes 3* and *4*). However, stable expression of a transgene can have multiple effects on the cells, and the increase in cytoplasmic p53 could potentially be caused by undetected adaptive mechanisms acquired during selection and stable expression of MSL2. To conclude that the cytoplasmic p53 detected in the U2OS-F-HA-MSL2 stable line is indeed caused by MSL2 expression and not by an undetected adaptive mechanism, we preformed RNA interference experiments to knock down the levels of F-HA-MSL2 in the stable line (Fig. 10*B*). Concomitant experiments were performed in parental U2OS cells to ensure that no additional off-target effects were induced by the siRNA treatment. Successful knockdown of the stably expressed F-HA-MSL2 was detected by Western blot with HA antibody (Fig. 10*B*, *upper panel*, *lanes 5* and *7*). Although knockdown of MSL2 had no detectable effect in the parental U2OS cells, reduction of MSL2 in the stable line significantly reduced the levels of cytoplasmic p53 detected in these cells (Fig. 10*B*, *lane 6*

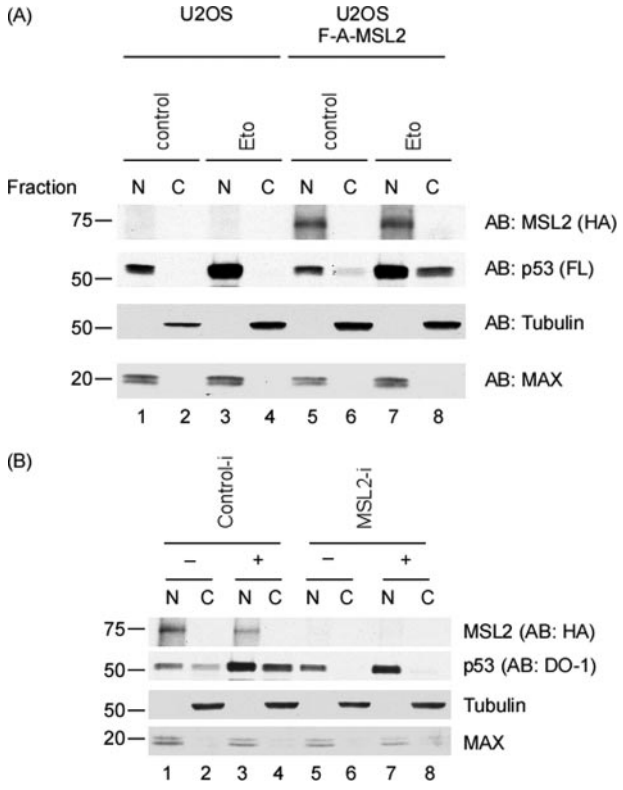

FIGURE 11. **Effect of stably expressed F-HA-MSL2 on p53 subcellular localization after DNA damage.** *A*, effect of etoposide treatment on p53 levels and subcellular localization in U2OS parental cells and U2OS-F-HA-MSL2 stable line. U2OS parental and U2OS-F-HA-MSL2 stable cells were treated with etoposide (*Eto*) for 6 h. Untreated control cells and etoposide-treated cells were fractionated, and nuclear (*N*) and cytoplasmic (*C*) fractions were analyzed by Western blot as indicated. *B*, effect of RNA interference-mediated knockdown of F-HA-MSL2 on p53 subcellular localization in U2OS-F-HA-MSL2 stable line after DNA damage. Stably expressed F-HA-MSL2 was knocked down by three rounds of transfection with control oligos (*lanes 1–4*) or MSL2-specific oligos (*lanes 5–8*). After knockdown, cells were split, and after 24 h they were treated with etoposide for 6 h prior to fractionation and analysis by Western blot as indicated. *AB*, antibody.

versus 8). The increase in cytoplasmic p53 in the stable line and the MSL2-siRNA-mediated reduction of the detected cytoplasmic p53 indicate that MSL2 is able to regulate changes in subcellular localization of endogenous p53.

Effect of Stably Expressed F-HA-MSL2 on p53 Subcellular Localization after DNA Damage—p53 levels are stabilized upon DNA damage, a process believed to depend primarily on inhibiting the p53-Mdm2 interaction and thereby preventing p53 ubiquitination by Mdm2 (4, 60). To determine what effect the expression of MSL2 might have on the stabilization and localization of endogenous p53, we treated U2OS parental cells and the U2OS-F-HA-MSL2 stable line with etoposide for 6 h to induce DNA damage (Fig. 11*A*). After etoposide treatment, untreated and treated cells were harvested and fractionated to determine the extent of p53 stabilization and subcellular localization. In parental U2OS cells, nuclear p53 was readily stabilized upon DNA damage, as expected (Fig. 11*A*, *lane 1 versus lane 3*). Under the conditions used for DNA damage treatment and fractionation, almost no cytoplasmic p53 was detected in the parental cells regardless of the treatment. As expected, nuclear p53 was readily stabilized by etoposide treatment in the U2OS-F-HA-MSL2 as well (Fig. 11*A*, *lane 5 versus lane 7*). Furthermore, the cytoplasmic p53 that can be detected in the MSL2 stable line was also stabilized by etoposide treatment (Fig. 11*A*, *lane 6 versus lane 8*), supporting the previously published notion that nuclear and cytoplasmic p53 can be stabilized independently (29). To demonstrate that the effects of DNA damage on stabilization and localization of p53 are MSL2-dependent, the stably expressed F-HA-MSL2 was knocked down by three round of transfection with MSL2-specific siRNA oligos prior to DNA damage treatment (Fig. 11*B*). Although treatment of cells transfected with control oligos (Fig. 11*B*, *lanes 1–4*) showed the same increases in both nuclear and cytoplasmic p53 as described in Fig. 11*A*, knockdown of the stably expressed F-HA-MSL2 (Fig. 11*B*, *lanes 5–8*) resulted in the reduction of cytoplasmic p53, as shown in Fig. 10*B*, and only nuclear p53 was stabilized by etoposide treatment. Together these data indicate that p53 localized in the cytoplasm due to MSL2-mediated ubiquitination can be stabilized by DNA damage and that MSL2 expression affects p53 localization but not p53 stabilization.

DISCUSSION

p53 plays a central role in determining cell fate after stress, with growth arrest and apoptosis the two major outcomes of p53 activation (1–3, 13, 14). Although growth arrest is induced predominantly through transcription of p53 target genes such as *p21* and *GADD45* (61), multiple mechanisms exist for p53-mediated apoptosis, including transcription of pro-apoptotic target genes (62) and activation of the mitochondrial apoptotic pathway (13, 15, 18). However, the exact contribution of these individual pathways remains unresolved (2, 13, 18). The role of Mdm2 in the regulation of p53-mediated apoptosis remains equally puzzling. The well established genetic data clearly identify Mdm2 as a negative regulator of p53 (39, 40). However, this negative regulation of p53 is somewhat at odds with convincing data that clearly demonstrate the role Mdm2 plays in promoting p53 cytoplasmic localization (28, 30) and subsequent p53-dependent pro-apoptotic activity (18, 27). The relationship between Mdm2 and p53 is extremely complicated because of the regulatory feedback loop that exists between the two and the fact that Mdm2-mediated ubiquitination of p53 can have multiple effects in the cell (4). A recent mechanistic study of the degradation-independent roles played by Mdm2-mediated ubiquitination of p53 revealed that ubiquitination does not affect tetramerization and oligomerization of p53 (63). That study demonstrated that ubiquitin-mediated repression of p53 transactivational activity by Mdm2 required not only its sequestration into the cytoplasm but also an inhibition of its sequence-specific binding activity. Additional mechanistic insights into the ubiquitin-mediated regulation of subcellular p53 localization were obtained by studying p53-ubiquitin fusion proteins (30). Monoubiquitination of p53 acts to expose a C-terminal nuclear export sequence and promotes the dissociation of Mdm2, thereby allowing further post-translational modifications of the C-terminal lysines, such as sumoylation, which promote nuclear export of p53 (30). Interestingly, stress-induced increases in cytoplasmic p53 have been attributed primarily to the stabilization of existing cytoplasmic p53 pools instead of the shuttling of nuclear p53 into the cytoplasm (18,

29). Careful fractionation experiments suggest that both nuclear and cytoplasmic p53 pools are stabilized independently. Stabilization of cytoplasmic p53 depends, at least in part, on allowing the accumulation of monoubiquitinated p53 in the cytoplasm. Monoubiquitination, stabilization, and subsequent localization to the mitochondria are thought to depend on Mdm2 activity, yet Mdm2 itself does not act as a shuttle for the mitochondrial localization of p53. This model depends on a delicate balance of Mdm2 levels in unstressed and stress-induced states. It will be interesting to see how MSL2, which was shown here to promote cytoplasmic p53 localization without affecting p53 stability, contributes to both steady state and stress-induced levels of cytoplasmic and mitochondrial p53 and whether MSL2 contributes to p53-dependent apoptosis.

In addition to the role played by MSL2 in establishing and maintaining cytoplasmic levels of wild type p53, MSL2 may help to explain the results obtained by p53 mutants with transactivation deficiencies such as $p53^{QS}$ and p53–6KR, which cannot be regulated by Mdm2 and yet retain significant apoptotic ability (43, 57). In the case of the $p53^{QS}$ mutant, early cell culture studies demonstrated that $p53^{QS}$ is able to trigger apoptosis in HeLa cells despite failing to significantly activate many of the relevant p53 target promoters, suggesting transactivation-independent ways for p53 to induce apoptosis (42). Recently, work conducted in H1299 cells showed that $p53^{QS}$ was able to promote expression of some pro-apoptotic target genes such as *PIDD* and *AIP1* and was able to induce apoptosis, although at a slower rate than wild type p53 (64). The study also reported that, even though many downstream apoptotic effectors are not induced by $p53^{QS}$, caspase-2 activation occurs, leading to cytochrome *c* release (64). Although MSL2 was shown to induce cytoplasmic localization of $p53^{QS}$, future studies may also focus on the regulation of some of these p53 target genes and the resulting activation of caspase-2 by MSL2. Such studies may help to dissect which role and to what extent individual pro-apoptotic functions of p53 contribute to the cellular responses to stress. Although the pro-apoptotic capability of the $p53^{QS}$ mutant was demonstrated quite early in cell lines, studies using transgenic animals initially suggested that cells carrying a $p53^{QS}$ mutant protein could not undergo damage-induced apoptosis (65). Two subsequent transgenic approaches, however, demonstrated that animals and cell lines derived from transgenic animals that carry the $p53^{QS}$ mutant do retain some of the transcriptional and pro-apoptotic capabilities, lending strong support to the early cell culture studies (43, 44). Cytoplasmic localization of $p53^{QS}$ was described in MEF cells derived from the $p53^{QS}$ transgenics upon stress induction (43), further supporting the requirement for additional factors other than Mdm2 for establishing cytoplasmic pools. Here, it has been shown that MSL2 promotes cytoplasmic localization of $p53^{QS}$ and p53–6KR mutants and that the changes in subcellular localization of p53 are independent of Mdm2. It will be of future interest to determine how MSL2 contributes to the regulation of $p53^{QS}$ both in animals and in cells lines derived from these mice.

Unlike Mdm2, MSL2 is an evolutionarily conserved protein (50). Lower organisms such as *D. melanogaster* and *Caenorhabditis elegans*, which lack Mdm2 but have conserved MSL2, have functional p53 that is critically involved in their stress-induced apoptotic response (66). It will be interesting to determine whether MLS2 orthologs play a role in regulating the subcellular localization of p53 in these organisms or whether MSL2 performs some of the other upstream regulatory functions that Mdm2 performs in mammals. An additional interesting aspect arises from the evolutionarily conserved presence of MSL2 and MOF in dosage compensation complexes (50). hMOF can acetylate p53 within the DNA-binding domain to specifically regulate its transcriptional activity on pro-apoptotic targets (53). Mutation of Lys-120 within p53 has been found in human tumors, and p53-K120R mutations selectively block transactivation of pro-apoptotic target genes (53). As MSL2 and MOF, two components of the dosage compensation complex, can regulate p53, it will be interesting to determine whether additional cross-talk between these two regulatory mechanisms exists.

Depending on which specific E3 ligase promotes the ubiquitination of p53, a different functional consequence arises, providing a basis for differential classification of these enzymes. The first class describes E3 ligases that can promote both mono- and polyubiquitination and thereby evoke differential functional consequences such as changes in subcellular localization, inhibition of DNA binding, or targeting for proteasomal degradation. Thus far, Mdm2 is the only p53-specific E3 ligase that has been found able to perform such differential regulation (4, 12, 67). Based on their ability to target p53 for degradation by polyubiquitination, ARF-BP1, COP-1, and Pirh2 comprise the second group of E3 ligases (4). Regulating subcellular localization by ubiquitination without affecting p53 stability, as shown here by MSL2, identifies a third class of functional consequences of p53 ubiquitination. The E4F1-mediated ubiquitination of p53, regulates transactivation, providing another example of specific functional consequences resulting from p53 ubiquitination. Together, these different classes of E3 ligases provide a regulatory network for p53 that is able to control a multitude of specific p53 functions. It will be of future interest to determine which E3 ligases act, under basal or stress-induced conditions, to regulate p53. Finally, although our study has identified MSL2 as an important ubiquitin ligase for Mdm2-independent cytoplasmic localization of p53, future studies will be required to address whether MSL2 can act as a regulator of p53-mediated apoptosis or other cytoplasmic p53 functions.

Acknowledgment—We thank Dr. John Lucchesi for reagents.

REFERENCES

1. Vousden, K. H., and Lane, D. P. (2007) *Nat. Rev. Mol. Cell Biol.* **8,** 275–283
2. Laptenko, O., and Prives, C. (2006) *Cell Death Differ.* **13,** 951–961
3. Toledo, F., and Wahl, G. M. (2006) *Nat. Rev. Cancer* **6,** 909–923
4. Brooks, C. L., and Gu, W. (2006) *Mol. Cell* **21,** 307–315
5. Kruse, J. P., and Gu, W. (2008) *Cell* **133,** 930–930 e931
6. Haupt, Y., Maya, R., Kazaz, A., and Oren, M. (1997) *Nature* **387,** 296–299
7. Kubbutat, M. H., Jones, S. N., and Vousden, K. H. (1997) *Nature* **387,** 299–303
8. Honda, R., Tanaka, H., and Yasuda, H. (1997) *FEBS Lett.* **420,** 25–27
9. Leng, R. P., Lin, Y., Ma, W., Wu, H., Lemmers, B., Chung, S., Parant, J. M., Lozano, G., Hakem, R., and Benchimol, S. (2003) *Cell* **112,** 779–791
10. Dornan, D., Bheddah, S., Newton, K., Ince, W., Frantz, G. D., Dowd, P.,

Koeppen, H., Dixit, V. M., and French, D. M. (2004) *Cancer Res.* **64,** 7226–7230
11. Chen, D., Kon, N., Li, M., Zhang, W., Qin, J., and Gu, W. (2005) *Cell* **121,** 1071–1083
12. Marine, J. C., Francoz, S., Maetens, M., Wahl, G., Toledo, F., and Lozano, G. (2006) *Cell Death Differ.* **13,** 927–934
13. Chipuk, J. E., and Green, D. R. (2006) *Cell Death Differ.* **13,** 994–1002
14. Fridman, J. S., and Lowe, S. W. (2003) *Oncogene* **22,** 9030–9040
15. Moll, U. M., Wolff, S., Speidel, D., and Deppert, W. (2005) *Curr. Opin. Cell Biol.* **17,** 631–636
16. Caelles, C., Helmberg, A., and Karin, M. (1994) *Nature* **370,** 220–223
17. Riley, T., Sontag, E., Chen, P., and Levine, A. (2008) *Nat. Rev. Mol. Cell Biol.* **9,** 402–412
18. Marchenko, N. D., and Moll, U. M. (2007) *Cell Cycle* **6,** 1718–1723
19. Marchenko, N. D., Zaika, A., and Moll, U. M. (2000) *J. Biol. Chem.* **275,** 16202–16212
20. Gilman, C. P., Chan, S. L., Guo, Z., Zhu, X., Greig, N., and Mattson, M. P. (2003) *Neuromolecular Med.* **3,** 159–172
21. Dumont, P., Leu, J. I., Della Pietra, A. C., III, George, D. L., and Murphy, M. (2003) *Nat. Genet.* **33,** 357–365
22. Mihara, M., Erster, S., Zaika, A., Petrenko, O., Chittenden, T., Pancoska, P., and Moll, U. M. (2003) *Mol. Cell* **11,** 577–590
23. Leu, J. I., Dumont, P., Hafey, M., Murphy, M. E., and George, D. L. (2004) *Nat. Cell Biol.* **6,** 443–450
24. Endo, H., Kamada, H., Nito, C., Nishi, T., and Chan, P. H. (2006) *J. Neurosci.* **26,** 7974–7983
25. Murphy, M. E., Leu, J. I., and George, D. L. (2004) *Cell Cycle* **3,** 836–839
26. Manfredi, J. J. (2003) *Mol. Cell* **11,** 552–554
27. Lohrum, M. A., Woods, D. B., Ludwig, R. L., Balint, E., and Vousden, K. H. (2001) *Mol. Cell. Biol.* **21,** 8521–8532
28. Li, M., Brooks, C. L., Wu-Baer, F., Chen, D., Baer, R., and Gu, W. (2003) *Science* **302,** 1972–1975
29. Marchenko, N. D., Wolff, S., Erster, S., Becker, K., and Moll, U. M. (2007) *EMBO J.* **26,** 923–934
30. Carter, S., Bischof, O., Dejean, A., and Vousden, K. H. (2007) *Nat. Cell Biol.* **9,** 428–435
31. Gu, J., Nie, L., Wiederschain, D., and Yuan, Z. M. (2001) *Mol. Cell. Biol.* **21,** 8533–8546
32. Nie, L., Sasaki, M., and Maki, C. G. (2007) *J. Biol. Chem.* **282,** 14616–14625
33. Tomita, Y., Marchenko, N., Erster, S., Nemajerova, A., Dehner, A., Klein, C., Pan, H., Kessler, H., Pancoska, P., and Moll, U. M. (2006) *J. Biol. Chem.* **281,** 8600–8606
34. Chipuk, J. E., and Green, D. R. (2004) *Cell Cycle* **3,** 429–431
35. Chipuk, J. E., Kuwana, T., Bouchier-Hayes, L., Droin, N. M., Newmeyer, D. D., Schuler, M., and Green, D. R. (2004) *Science* **303,** 1010–1014
36. Speidel, D., Helmbold, H., and Deppert, W. (2006) *Oncogene* **25,** 940–953
37. Tasdemir, E., Maiuri, M. C., Galluzzi, L., Vitale, I., Djavaheri-Mergny, M., D'Amelio, M., Criollo, A., Morselli, E., Zhu, C., Harper, F., Nannmark, U., Samara, C., Pinton, P., Vicencio, J. M., Carnuccio, R., Moll, U. M., Madeo, F., Paterlini-Brechot, P., Rizzuto, R., Szabadkai, G., Pierron, G., Blomgren, K., Tavernarakis, N., Codogno, P., Cecconi, F., and Kroemer, G. (2008) *Nat. Cell Biol.* **10,** 676–687
38. Le Cam, L., Linares, L. K., Paul, C., Julien, E., Lacroix, M., Hatchi, E., Triboulet, R., Bossis, G., Shmueli, A., Rodriguez, M. S., Coux, O., and Sardet, C. (2006) *Cell* **127,** 775–788
39. Montes de Oca Luna, R., Wagner, D. S., and Lozano, G. (1995) *Nature* **378,** 203–206
40. Jones, S. N., Roe, A. E., Donehower, L. A., and Bradley, A. (1995) *Nature* **378,** 206–208
41. Lin, J., Chen, J., Elenbaas, B., and Levine, A. J. (1994) *Genes Dev.* **8,** 1235–1246
42. Haupt, Y., Rowan, S., Shaulian, E., Vousden, K. H., and Oren, M. (1995) *Genes Dev.* **9,** 2170–2183
43. Jimenez, G. S., Nister, M., Stommel, J. M., Beeche, M., Barcarse, E. A., Zhang, X. Q., O'Gorman, S., and Wahl, G. M. (2000) *Nat. Genet.* **26,** 37–43
44. Johnson, T. M., Hammond, E. M., Giaccia, A., and Attardi, L. D. (2005) *Nat. Genet.* **37,** 145–152
45. Freedman, D. A., Wu, L., and Levine, A. J. (1999) *CMLS Cell. Mol. Life Sci.* **55,** 96–107
46. Zhang, Y., and Xiong, Y. (2001) *Cell Growth Differ.* **12,** 175–186
47. Liang, S. H., and Clarke, M. F. (1999) *J. Biol. Chem.* **274,** 32699–32703
48. Li, M., Luo, J., Brooks, C. L., and Gu, W. (2002) *J. Biol. Chem.* **277,** 50607–50611
49. Mendjan, S., and Akhtar, A. (2007) *Chromosoma* (*Berl.*) **116,** 95–106
50. Smith, E. R., Cayrou, C., Huang, R., Lane, W. S., Cote, J., and Lucchesi, J. C. (2005) *Mol. Cell. Biol.* **25,** 9175–9188
51. Rea, S., Xouri, G., and Akhtar, A. (2007) *Oncogene* **26,** 5385–5394
52. Marin, I. (2003) *J. Mol. Evol.* **56,** 527–539
53. Sykes, S. M., Mellert, H. S., Holbert, M. A., Li, K., Marmorstein, R., Lane, W. S., and McMahon, S. B. (2006) *Mol. Cell* **24,** 841–851
54. Fang, S., Lorick, K. L., Jensen, J. P., and Weissman, A. M. (2003) *Semin. Cancer Biol.* **13,** 5–14
55. Pickart, C. M. (2001) *Annu. Rev. Biochem.* **70,** 503–533
56. Hicke, L., and Dunn, R. (2003) *Annu. Rev. Cell Dev. Biol.* **19,** 141–172
57. Feng, L., Lin, T., Uranishi, H., Gu, W., and Xu, Y. (2005) *Mol. Cell. Biol.* **25,** 5389–5395
58. Nakamura, S., Roth, J. A., and Mukhopadhyay, T. (2000) *Mol. Cell. Biol.* **20,** 9391–9398
59. Rodriguez, M. S., Desterro, J. M., Lain, S., Lane, D. P., and Hay, R. T. (2000) *Mol. Cell. Biol.* **20,** 8458–8467
60. Brooks, C. L., and Gu, W. (2003) *Curr. Opin. Cell Biol.* **15,** 164–171
61. Vogelstein, B., Lane, D., and Levine, A. J. (2000) *Nature* **408,** 307–310
62. Yu, J., and Zhang, L. (2005) *Biochem. Biophys. Res. Commun.* **331,** 851–858
63. Brooks, C. L., Li, M., and Gu, W. (2007) *J. Biol. Chem.* **282,** 22804–22815
64. Baptiste-Okoh, N., Barsotti, A. M., and Prives, C. (2008) *Proc. Natl. Acad. Sci. U. S. A.* **105,** 1937–1942
65. Chao, C., Saito, S., Kang, J., Anderson, C. W., Appella, E., and Xu, Y. (2000) *EMBO J.* **19,** 4967–4975
66. Lu, W. J., and Abrams, J. M. (2006) *Cell Death Differ.* **13,** 909–912
67. Clegg, H. V., Itahana, K., and Zhang, Y. (2008) *Cell Cycle* **7,** 287–292